

# Responses of Medial Rectus Motoneurons in Monkeys with Strabismus

Anand C. Joshi and Vallabh E. Das

**PURPOSE.** Monkeys reared under conditions of alternating monocular occlusion during their first few months of life show large horizontal strabismus, “A” patterns, and dissociated vertical deviation. “A” patterns manifest as an inappropriate horizontal component in the deviated eye during vertical eye movements (cross-axis movement). The objective of this study was to investigate response properties of medial rectus motoneurons (MRMNs) in relation to strabismus properties.

**METHODS.** Burst-tonic activity of 21 MRMNs in the oculomotor nucleus were recorded from two monkeys with exotropia as they performed horizontal and vertical smooth pursuit (0.2 Hz,  $\pm 10^\circ$ ) under monocular viewing conditions. Neuronal responses and horizontal component of eye movements were used to identify regression coefficients in a first-order model for each tracking condition.

**RESULTS.** Comparison of position, velocity, and constant parameter coefficients, estimated from horizontal tracking data with either eye viewing, showed no significant differences ( $P > 0.07$ ), indicating that neuronal activity could account for the horizontal misalignment. Comparison of the position, velocity, and constant parameter coefficients estimated from horizontal tracking and the cross-axis condition showed no significant differences ( $P > 0.07$ ), suggesting that motoneuron activity could account for most of the inappropriate horizontal cross-axis movement observed in the covered eye during vertical smooth pursuit.

**CONCLUSIONS.** These data suggest that, in animals with sensory-induced strabismus, central innervation to extraocular muscles is responsible for setting the state of strabismus. Mechanical factors such as muscle length adaptation (for horizontal misalignment) and pulley heterotopy or static torsion (for “A” patterns) likely do not play a major role in determining properties in a sensory-induced strabismus. (*Invest Ophthalmol Vis Sci.* 2011;52:6697–6705) DOI:10.1167/iovs.11-7402

Disrupting binocular vision during the critical period of development in an infant monkey or human leads to permanent strabismus.<sup>1,2</sup> In nonhuman primate models for strabismus, disruption of binocular vision can be achieved by surgical or sensory methods.<sup>3–5</sup> We have shown that monkeys reared for the first 4 months of life under conditions of daily

alternating monocular occlusion (AMO) develop a large horizontal misalignment with A/V patterns and a dissociated vertical deviation (DVD) that varies with horizontal gaze position.<sup>2</sup> During eye-movement tasks, the A/V patterns and DVD manifest as an inappropriate eye-movement component in the plane orthogonal to the visually guided movement (cross-axis movement) and is observed only in the nonfixating eye. Other strabismus properties of the AMO monkeys include alternating fixation and saccade disconjugacy.<sup>6,7</sup>

Previously, we reported results from neural recordings of vertical burst-tonic motoneurons in the oculomotor nucleus (OMN) of the strabismic monkeys.<sup>8</sup> Our data showed that activity of vertical motoneurons was modulated during vertical tracking with either eye fixating the target (as would be expected) and also similarly modulated in correlation with the inappropriate vertical component of eye movement observed in the nonfixating eye during horizontal tracking. Therefore, these data for the first time showed a neural correlate to a disorder of binocular coordination in a strabismic monkey. However, the data from vertical motoneurons were pertinent only to the observation of DVD and its variation with horizontal gaze position. Strabismic monkeys, like many strabismic humans, also show “A” or “V” patterns (variation of horizontal strabismus angle with vertical gaze position). It is not known whether A/V patterns also might have a neural basis. Alternatively, mechanical factors such as a change in extraocular muscle (EOM) pulling direction either due to pulley problems or a static torsional offset could play a role in producing the A/V pattern.<sup>9–11</sup>

It may be that when the etiology of the strabismus is sensory, then all strabismus phenomena including the horizontal misalignment have a neural basis.<sup>12</sup> However, mechanical factors at the level of the EOM could also be critical in determining the state of horizontal misalignment. Scott<sup>13</sup> first described a phenomenon called “muscle length adaptation” when studying monkey EOM after resection surgery. He observed that sarcomeres were initially shortened after surgery, but after 6 to 8 weeks appeared to have returned to their original length. Although the observations made were after surgical intervention, an important implication of this study was that muscle length could adapt to the state of the strabismus.<sup>14,15</sup> It could then be argued that, whatever is the etiology of the strabismus (mechanical or neural), once the muscle length is adapted (steady state strabismus), the apparent “overaction” or “underaction” of individual EOMs is driven by altered muscle lengths. In the case of a sensory-induced strabismus (as in the AMO monkey) the unbalanced neuronal drive to the medial and lateral recti that initially drove the strabismus could revert to a “normal” value once the muscle lengths are adapted to a new state corresponding to the strabismus angle.

The goal of the present study was therefore to focus on responses of horizontal (medial rectus) motoneurons in the OMN and examine their responses in relation to the state of strabismus. Two primary questions were identified: (1) What is the relationship between medial rectus motoneuron (MRMN)

From the College of Optometry, University of Houston, Houston, Texas.

Supported in part by National Institutes of Health Grant R01-EY015312 (VED); University of Houston, College of Optometry Core Grant P30 EY07551; and Yerkes Center Base Grant RR00165, Division of Research Resources.

Submitted for publication February 15, 2011; revised May 31 and June 22, 2011; accepted June 23, 2011.

Disclosure: A.C. Joshi, None; V.E. Das, None

Corresponding author: Vallabh E. Das, College of Optometry, University of Houston, 505 J Davis Armistead Building, 4901 Calhoun Rd, Houston, TX 77204; vdas@optometry.uh.edu.

activity and the state of horizontal misalignment? These data could be used either to support or to argue against muscle length adaptation in a sensory-induced strabismus. (2) Are MRMN responses correlated with the horizontal component of cross-axis movements, thereby providing justification for a neural source for “A” and “V” patterns? Some of these data were previously presented in abstract form (Joshi AC, Das VE. *IOVS* 2011;52:ARVO E-Abstract 4689).

## METHODS

### Subjects and Rearing Paradigms

Behavioral and neurophysiological data were collected from two juvenile rhesus (*Macaca mulatta*) monkeys (ages, 5 and 7 years; weights, 7 and 10 kg) with exotropia. Strabismus was induced by disrupting development of binocular vision during infancy using a daily alternating monocular occlusion (AMO) method. In the AMO rearing paradigm, within the first 24 hours after birth, an occluding patch (dark contact lenses for the monkeys in this study) was placed in front of one eye for a period of 24 hours and thereafter switched to the fellow eye for the next 24 hours. The patch was alternated daily for a period of 4 months. For additional details on AMO rearing and strabismus properties in the AMO monkey, refer to our previous publications (Das VE, et al. *IOVS* 2007;48:ARVO E-Abstract 5273).<sup>2,5,6,8,16</sup>

### Surgical Procedures

After special rearing, the AMO animals were allowed to grow with unrestricted vision, until they were approximately 3 to 4 years of age, before behavioral and neurophysiological experiments were conducted. Sterile surgical procedures performed under aseptic conditions using isoflurane anesthesia (1.25% to 2.5%) were used to stereotactically implant a head stabilization post and a recording chamber. The recording chamber was a 21-mm-diameter titanium cylinder implanted at a stereotaxic location 3-mm anterior, 1-mm lateral, and at a 20° angle to the sagittal plane. This chamber placement allowed full access to both OMN. During the same surgical procedure, a scleral search coil was implanted in one eye according to procedures laid out by Judge et al.<sup>17</sup> Later, in a second surgery, a second scleral search coil was implanted in the other eye. All procedures were performed in strict compliance with National Institutes of Health and the Association for Research in Vision and Ophthalmology guidelines, and the protocols were reviewed and approved by the Institutional Animal Care and Use Committees.

### Experimental Paradigms and Data Acquisition

Binocular eye, target, and unit data were collected as the animals performed smooth-pursuit tracking of a horizontally or vertically moving sinusoidal target (0.2 Hz,  $\pm 10$ – $15^\circ$ ) under monocular right eye or left eye viewing conditions. Binocular eye position was measured using the magnetic search coil method (Angle-Meter; Primelec Industries, Regensdorf, Switzerland). Eye coil signals were calibrated under monocular viewing conditions by rewarding the monkey for looking within a 2–3° window surrounding a 1° diameter target spot that was rear projected on a tangent screen 60 cm away from the animal. Visual stimuli were generated under computer control using a stimulus generator graphics card installed in a PC (VSG2/5 for Windows; Cambridge Research Systems, Kent, UK). Binocular eye and target position feedback signals were processed with antialiasing filters at 400 Hz before digitization at 1 kHz with 12-bit precision (AlphaLab System; Alpha Omega Engineering, Nazareth Illit, Israel).

Single-unit data were acquired using epoxy-coated tungsten electrodes (1–5 M $\Omega$ ; FHC Inc., Brunswick, ME). The OMN was identified by its stereotaxic location and characteristic “beehive” sound of the burst-tonic (BT) cells during eye movements made in the on-direction of the cells. Thus left BT cells were those in the right OMN and were sensitive to leftward eye movements (vice versa for right BT cells). During initial

electrode penetrations, we mapped the rostrocaudal extent of the OMN and established the midline. Raw spike data were acquired in our data acquisition system at a sampling rate of 32 kHz. Spike sorting was performed offline using a template-matching algorithm (Spike2 software; Cambridge Electronic Design, Cambridge, UK) and timestamps corresponding to each action potential were generated and used to compute the neuronal firing rate.

## Data Analysis

Data analysis was performed with custom software routines (MATLAB; The MathWorks, Natick, MA). Velocity arrays were generated by digital differentiation of position arrays using a central point difference algorithm. Unit response was represented as a spike density function that was generated by convolving timestamps with a 20-ms Gaussian.<sup>18</sup> Eye, target, and the unit spike density function data were filtered using an 80-point finite impulse response digital filter with a pass band of 0 to 80 Hz. Saccades were removed from the sinusoidal tracking data using a 50°/s velocity criterion and corresponding spike data were also removed. This was deemed necessary because motoneuron position and velocity sensitivity measures tend to differ for saccadic and smooth-pursuit eye movements.<sup>19</sup> Both monkeys exhibited a small latent nystagmus with frequency of 1.5–2 Hz and velocity of approximately 1.5°/s for S1 and a frequency <1 Hz and velocity <1°/s for S2. The quick phases of the latent nystagmus were generally of lower velocity than that of the saccade threshold and so were not removed from the data.

In the first part of the analysis, used to determine whether static eye misalignment was encoded in motoneuron responses, averaged data from multiple cycles during which the animal was performing smooth-pursuit tracking of the horizontally moving sinusoidal target with either the left eye or the right eye viewing was used to identify coefficients ( $K$ ,  $R$ ,  $C$ ) in a first-order model:

$$FR(t) = KE(t) + RE'(t) + C \quad (1)$$

In this model,  $FR(t)$  is the estimated neuronal firing rate,  $E(t)$  is the horizontal position of the eye that the neuron projects to (right eye for left BT motoneurons in the right OMN and left eye for right BT motoneurons in the left OMN), and  $E'(t)$  is the corresponding horizontal eye velocity. It is possible that some of the cells in our sample are oculomotor interneurons (OINs) that project from the OMN to the contralateral abducens nucleus. The density of OINs within the OMN is rather low. In a study that used antidromic activation methods to unequivocally identify the OIN, the investigators encountered only 18 OINs in a sample of 438 neurons in the OMN. Importantly, the same study showed that these interneurons show response properties very similar to those of the MRMN.<sup>20</sup> Therefore the presence of a few OINs in our data set is unlikely to have any implication on data interpretation and so we did not attempt to identify them. Model fitting was performed using the “nlinfit” function (Matlab). For each regression coefficient, 95% confidence intervals (CIs) were developed using a bootstrap resampling method similar to that described by Sylvestre and Cullen.<sup>21</sup> The bootstrap method involved generating 1000 new data sets for each cell via random resampling with replacement of the sinusoidal tracking data. Regression coefficients [Eq. 1] of the model were developed from each of the 1000 data sets, resulting in the generation of a probability density function for each coefficient; the mean and SDs of each coefficient were thus calculated. The regression coefficient was determined to be significant if the 95% CI did not overlap with zero. For each fit, the coefficient of determination (CD) measure was used to determine the goodness-of-fit. Statistical analysis involved performing a pairwise comparison of each regression coefficient in the two horizontal tracking conditions for the entire cell sample.

The second part of analysis was used to determine whether the inappropriate horizontal cross-axis component observed in the non-viewing eye during vertical smooth pursuit was driven by neural

activity. For this analysis, a horizontal tracking data set was generated by combining horizontal eye data from the right eye and left eye viewing horizontal smooth-pursuit tasks, and a cross-axis data set was generated by combining the horizontal eye data from the right eye and left eye viewing vertical smooth-pursuit tasks. Thereafter, we estimated coefficients in a fully binocular model with the following structure:

$$FR(t) = K_i E_i(t) + R_i E_i'(t) + K_c E_c(t) + R_c E_c'(t) + C \quad (2)$$

In this model, subscripts “i” and “c” refer to the ipsilateral and contralateral eye components. Our rationale for using a fully binocular model for this analysis is based on findings in normal monkey studies by Zhou and King<sup>22</sup> and later by Cullen and colleagues.<sup>21,23</sup> These studies showed that, although MRMNs in the OMN and LRMNs in the abducens nucleus project directly to the ipsilateral eye muscle (and therefore would be expected to encode only movement of the eye to which they project), paradoxically they also encode movements of the fellow eye. The exact significance of the contralateral eye encoding is still unresolved. A subjective examination of our data during the horizontal cross-axis conditions (vertical smooth pursuit during either left or right eye viewing) showed that many cells in the sample were indeed modulated during both the right eye and left eye viewing conditions, thereby showing evidence for binocular encoding. We therefore decided that using a binocular model structure to estimate coefficients for all the cells in our sample would be the most objective method for this analysis.

Cells for which any of the model parameters for a particular eye were not significant (95% CI obtained from bootstrap method overlapped zero) were classified as monocular cells and the monocular model from equation 1 was reapplied to obtain the final position and velocity coefficients. Statistical testing for the second analysis involved performing a pairwise comparison of regression coefficients ( $K$ ,  $R$ , and  $C$ ) in the horizontal tracking data set versus cross-axis data set.

## RESULTS

### Eye Alignment and Cross-Axis Movements in Monkeys with Strabismus

Figure 1 illustrates a Hess-type representation showing eye misalignment during monocular horizontal or vertical smooth pursuit with either the right eye viewing (left column) or left eye viewing (right column) from monkey S1 (top row) and monkey S2 (bottom row). Both the animals showed exotropia, as indicated by the

abducted position of the left eye (blue trace) during the right eye viewing condition and the abducted position of the right eye (red trace) during the left eye viewing condition. An “A” pattern is observed in both the animals, as indicated by the change in the horizontal position of the nonviewing eye during vertical tracking. Finally, the two animals also show DVD as indicated by the upward shift in the nonviewing eye for both right eye and left eye viewing conditions and at all the horizontal gaze eccentricities. These are similar to strabismic properties that we have described earlier in other AMO monkeys,<sup>2</sup> although the degree of “A” patterns and therefore the magnitude of horizontal cross-axis movements was relatively small in animal S1. In Figure 2, we show a time view of horizontal or vertical smooth-pursuit eye movements in animal S2 during monocular left eye viewing. During horizontal tracking (Figs. 2B, 2D), there is an inappropriate vertical component only in the nonviewing right eye (red trace) and similarly during vertical tracking (Figs. 2A, 2C), there is an inappropriate horizontal component only in the nonviewing right eye.

### Analysis of Medial Rectus Motoneurons during Horizontal Smooth Pursuit

We recorded from 21 MRMNs in the two strabismic animals. Of these, 11 were from animal S1 and 10 were from S2. Fourteen of 21 cells were right-BT motoneurons (i.e., increased activity for rightward positions) and the rest were left-BT.

The first part of the analysis was to determine whether motoneuron responses encode the state of eye misalignment. To this end, we compared the activity of MRMNs during horizontal smooth pursuit with either eye viewing. Figure 3 shows data from a sample right BT motoneuron (modulated for rightward eye movements and projecting to the left eye medial rectus muscle) during the two tracking tasks. Data in Figures 3A and 3B show that the neuronal response is well correlated with the horizontal component of left eye movements during horizontal smooth pursuit with either eye fixing. When the animal is viewing with the right eye (Fig. 3B), the left eye is deviated toward the left due to the exotropia. The lower baseline activity of the cell in this condition accounts for the leftward deviation of the left eye. For each cell in our sample, we developed regression fits to relate motoneuron activity to movement of the ipsilateral eye [see Methods, Eq. 1]. The fit equations for the sample cell in Figure 3 are

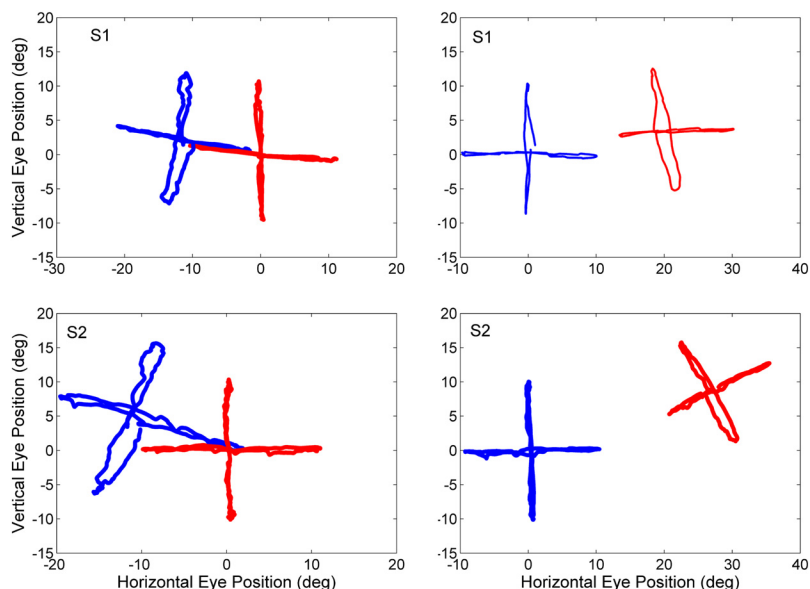


**FIGURE 1.** Eye misalignment patterns observed during horizontal and vertical smooth pursuit under monocular viewing conditions (*Left*: right eye viewing; *Right*: left eye viewing). In this and other plots upward and rightward eye positions are positive. Left eye data are shown in *blue*, whereas right eye data are *red*. Both animals showed significant horizontal misalignment (exotropia) that varied with vertical gaze.



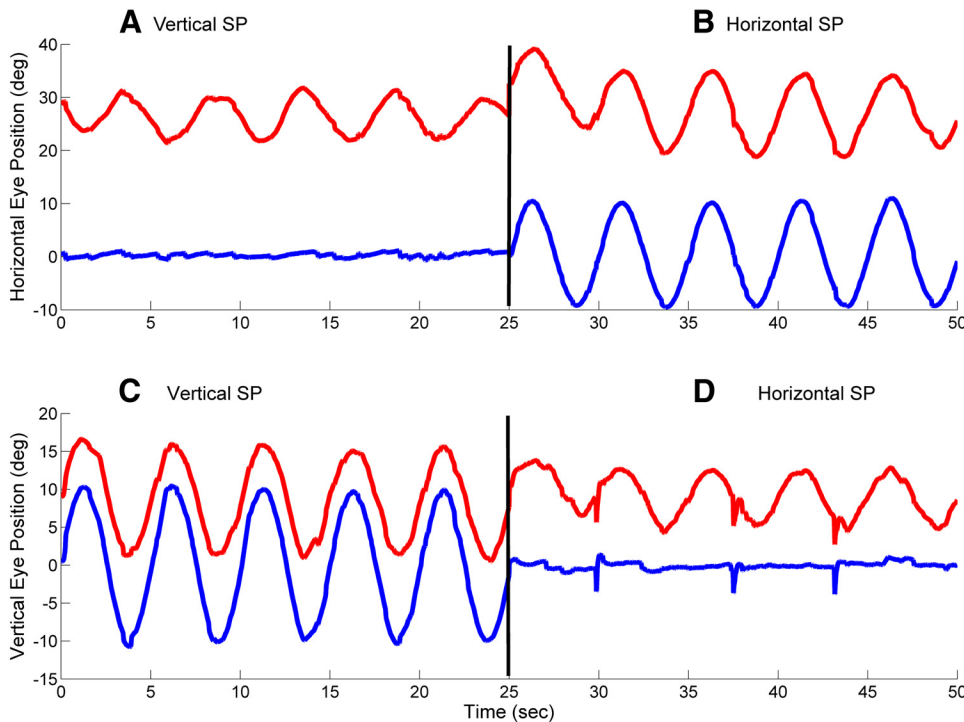
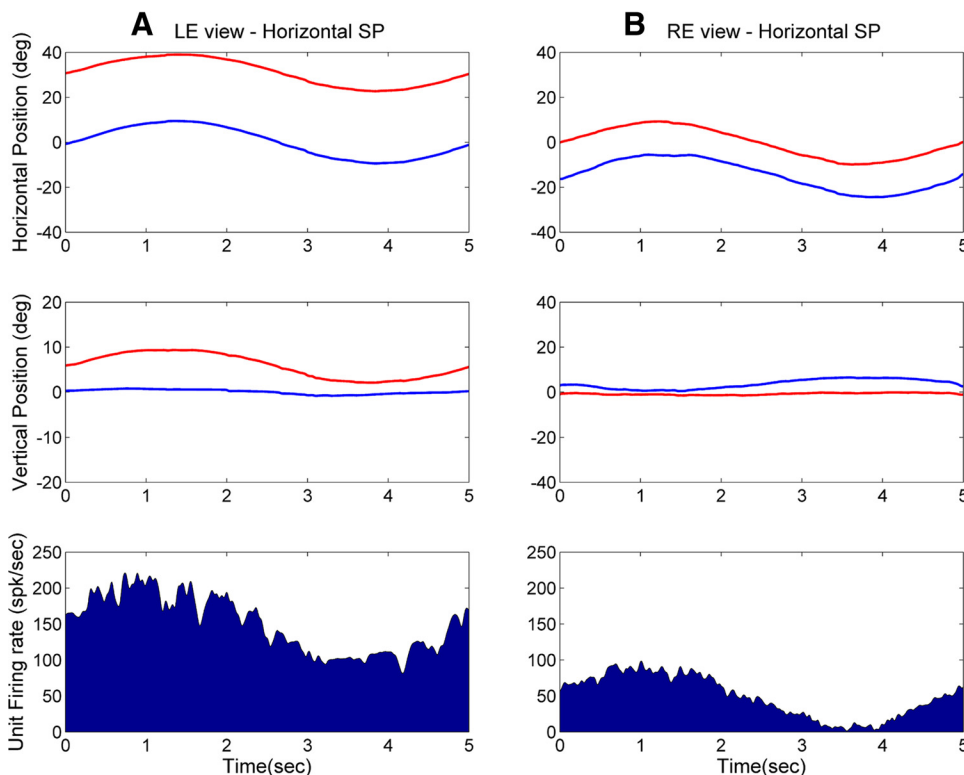


**FIGURE 2.** Plot showing raw eye movement data in animal S2 during horizontal and vertical smooth pursuit (0.2 Hz,  $\pm 10^\circ$ ), left eye viewing. The viewing eye (left eye, blue trace) makes a pure horizontal or vertical tracking eye movement. The non-viewing eye (right eye, red trace) shows an inappropriate cross-axis component, that is, inappropriate horizontal eye movement during vertical smooth pursuit (A) and inappropriate vertical eye movement during horizontal smooth pursuit (D). The animal exhibits a small latent nystagmus as seen most clearly on the horizontal left eye trace in (A).

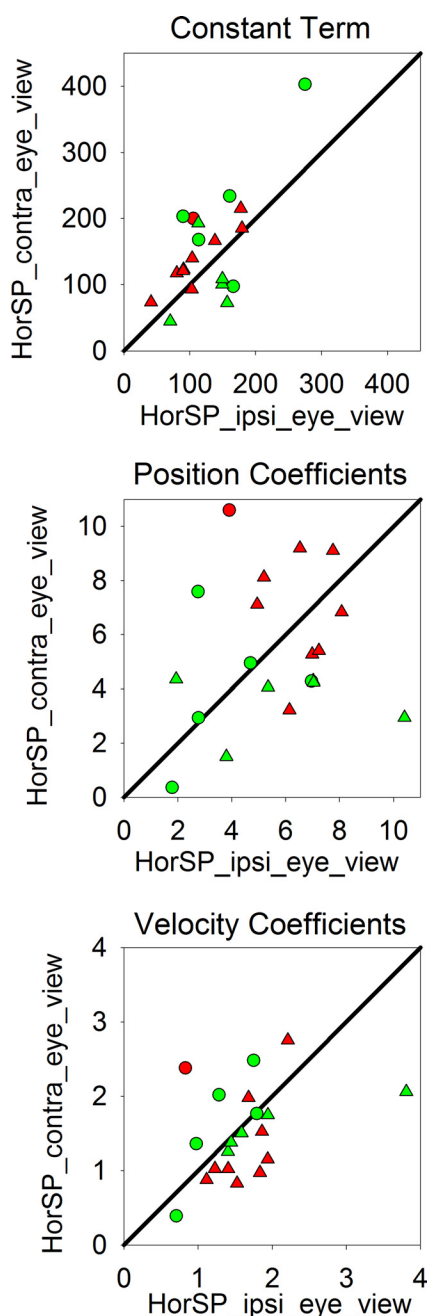
provided in the legend. In the fit equation,  $E(t)$  refers to position of the left eye,  $E'(t)$  refers to velocity of the left eye, and the constant terms signifies the firing rate of the motoneuron during fixation of a straight-ahead target at a 60-cm viewing distance.

Figure 4 shows comparative plots of position and velocity sensitivities and the constant term under the two horizontal tracking conditions for all cells in the sample. The  $x$ -axis in

Figure 4 shows the coefficient estimate for the horizontal tracking condition wherein the eye to which the neuron projects is the fixating eye (HorSP\_ipsi\_eye\_view; Fig. 3A) and the  $y$ -axis shows the coefficient estimates for the horizontal tracking condition wherein the eye to which the neuron projects is occluded (HorSP\_contra\_eye\_view; Fig. 3B). All the plots in Figure 4 show data distributed around the unity line, suggesting that the neuronal responses well encode both the state of



**FIGURE 3.** Single-unit activity in an example right burst-tonic cell (RTBT) motoneuron recorded from the left OMN and projecting to the left eye in S2. *Top and middle rows* show the averaged horizontal and vertical eye movements from both eyes (right eye, red trace; left eye, blue trace). The *bottom row* shows the associated neuronal activity. The neuronal activity is correlated with horizontal movements of the left eye for horizontal smooth pursuit with either eye viewing. There is a decrease in baseline activity of the cell during right eye viewing because the left eye is deviated to the left. Fit equations in the two tracking conditions are (A):  $FR(t) = 5.35E(t) + 1.41E'(t) + 150$ . (B)  $FR(t) = 4.06E(t) + 1.25E'(t) + 109$ .



**FIGURE 4.** Comparison of position sensitivity ( $K$ ), velocity sensitivity ( $R$ ), and constant term ( $C$ , signifying neuronal response when fixating a straight-ahead stationary target at  $0^\circ$ ) during horizontal tracking under left and right eye viewing conditions. On the  $x$ -axis is the estimated value during horizontal smooth pursuit when the eye to which the neuron projects is viewing the target; on the  $y$ -axis is the estimated value during horizontal smooth pursuit when the eye to which the neuron projects is the nonfixating eye. Note that for sake of simplicity of illustration, the parameter estimates are plotted without signs; otherwise, left-BT motoneurons would have negative parameter estimates. In this figure and in Figure 6, the circles denote left burst-tonic cells (LTBTs), whereas the triangles denote RTBTs. Cells recorded from monkey S1 are shown in red and cells recorded from monkey S2 are shown in green.

static misalignment and the dynamic horizontal eye movements. Pairwise comparison ( $t$ -test) of the model coefficients showed no significant difference in position ( $P = 0.74$ ), velocity ( $P = 0.55$ ), and constant term ( $P = 0.07$ ) for the two

horizontal tracking conditions. Population averages are listed in Table 1.

### Analysis of Medial Rectus Motoneurons during Vertical Smooth Pursuit

The second part of the analysis was to determine whether MRMNs could be driving the inappropriate horizontal cross-axis movement observed in the covered eye during vertical smooth pursuit (Fig. 2). Figure 5 shows the data from a sample right BT neuron in monkey S2 during the four tracking conditions. In this example, neural activity was correlated with rightward movement of the left eye whether it is associated with the horizontal tracking task (Figs. 5A, 5B) or an inappropriate horizontal movement of the left eye (cross-axis component) during vertical tracking with the right eye viewing (Fig. 5D). Interestingly, modulation of neuronal activity was also observed during vertical smooth pursuit with the left eye viewing (Fig. 5C). Since horizontal movements are observed only in the covered right eye, this activity must be related to the inappropriate horizontal cross-axis movement in the right eye. Thus it appears that this cell shows binocular encoding (i.e., it encodes horizontal movements of both the left [ipsilateral] and right [contralateral] eye).

We therefore decided that it was necessary to use a fully binocular model on all our cells to compare neuronal responses during horizontal tracking and cross-axis conditions. Model fits were developed for the horizontal tracking data set (e.g., combining Fig. 5A and Fig. 5B) and the cross-axis tracking data set (e.g., combining Fig. 5C and Fig. 5D). For the example cell in Figure 5, the model fit equations for the horizontal tracking and for the horizontal cross-axis movements during vertical tracking are in the legend. Five of 21 cells in our sample were eliminated because the regression fit for the horizontal cross-axis movement during vertical tracking had poor coefficient of determination (mean  $CD = 0.4$ ) and so the parameter estimates for these cells were not reliable. Four of the rejected cells were from S1, who displayed a significantly smaller cross-axis component (peak to peak value of  $2\text{--}3^\circ$ ) compared with S2 (peak to peak value of  $8\text{--}10^\circ$ ) for the vertical smooth-pursuit task. The single cell eliminated from animal S2 was rejected because the neural response during vertical smooth pursuit was too noisy to obtain a reliable regression fit. Of the remaining 16 cells, 7 were identified as monocular cells (all showed coding of the ipsilateral eye; contralateral eye coefficients were not significant) and the monocular model fit coefficients were estimated [Eq. 1]. The remaining cells (57%) were classified as binocular cells [Eq. 2].

Figure 6 shows comparative plots of the ipsilateral model coefficients for the cell sample. Pairwise comparison of the coefficients obtained for the fits during these conditions showed no statistical difference for the position ( $P = 0.16$ ), velocity ( $P = 0.07$ ), and constant term ( $P = 0.43$ ). Population averages for this comparison are listed in Table 2. Table 2 also includes population means of the contralateral eye coefficients. We also found no statistically significant differences in the contralateral eye position and velocity coefficients for the binocular cells (position coefficient  $K_c$ :  $P = 0.2$ ; velocity coefficient  $R_c$ :  $P = 0.52$ ) in the horizontal tracking and horizontal cross-axis movement conditions. The overall results obtained with the MRMNs are similar to the previously published observations for the vertical motoneurons,<sup>8</sup> supporting the hypothesis that the inappropriate horizontal cross-axis component observed during vertical tracking has a neural origin.

### DISCUSSION

Very little is known about how patterns of neural activity determine various strabismus oculomotor properties including the horizontal misalignment, A/V patterns, and DVD.<sup>12</sup> Previous work to

TABLE 1. Population Characteristics of MRMNs during Horizontal Tracking (mean ± standard deviation)

Parameter	HorSP_ipsi_eye_view	HorSP_contra_eye_view
Position coefficient, <i>K</i>	5.57 ± 2.26	5.32 ± 2.68
Velocity coefficient, <i>R</i>	1.62 ± 0.65	1.52 ± 0.62
Constant, <i>C</i>	127.64 ± 51.62	152.86 ± 79.4
Coefficient of Determination, CD	0.85 ± 0.16	0.86 ± 0.13

quantify the neuronal responses of motoneurons in primates with strabismus was focused on the vertical OMN and showed that the changes in vertical misalignment (DVD) with horizontal gaze indeed has a neural origin and is not due to problems in the periphery.<sup>8</sup> In this study we focused on MRMNs and attempted to identify relationships between horizontal motoneuron activity and horizontal misalignment and “A” patterns. Our data show that activity of horizontal motoneurons is responsible for setting the state of horizontal eye misalignment and that horizontal motoneuron activity also drives the inappropriate horizontal cross-axis movement observed during vertical tracking.

Relationship between MRMN Activity and Horizontal Misalignment

The relative roles of EOM and neural drive in setting the steady state strabismus angle are not clear. When the initial insult is a

sensory breakdown of binocular vision, then clearly errant signals from the brain in the form of unbalanced neural innervation of the medial and lateral rectus muscles of an eye must drive the induction of strabismus. However, do these signals also help maintain the steady state strabismus? There is some evidence to suggest that EOM might take over the role of maintaining the strabismic state.<sup>24,25</sup> Scott<sup>13</sup> performed an experiment in which he induced exotropia in adult monkeys by suturing the globe to the orbital wall. Monkeys that were examined soon after the procedure showed increased sarcomere length and muscle length of the medial rectus and shortened sarcomere length and muscle length of the lateral rectus. However, in a monkey examined 2 months later, the sarcomere lengths in the treated eye were similar to those of the control eye, although the muscle lengths themselves were altered. This result has often been used to argue that, after strabismus surgery, muscles remodel themselves such that their

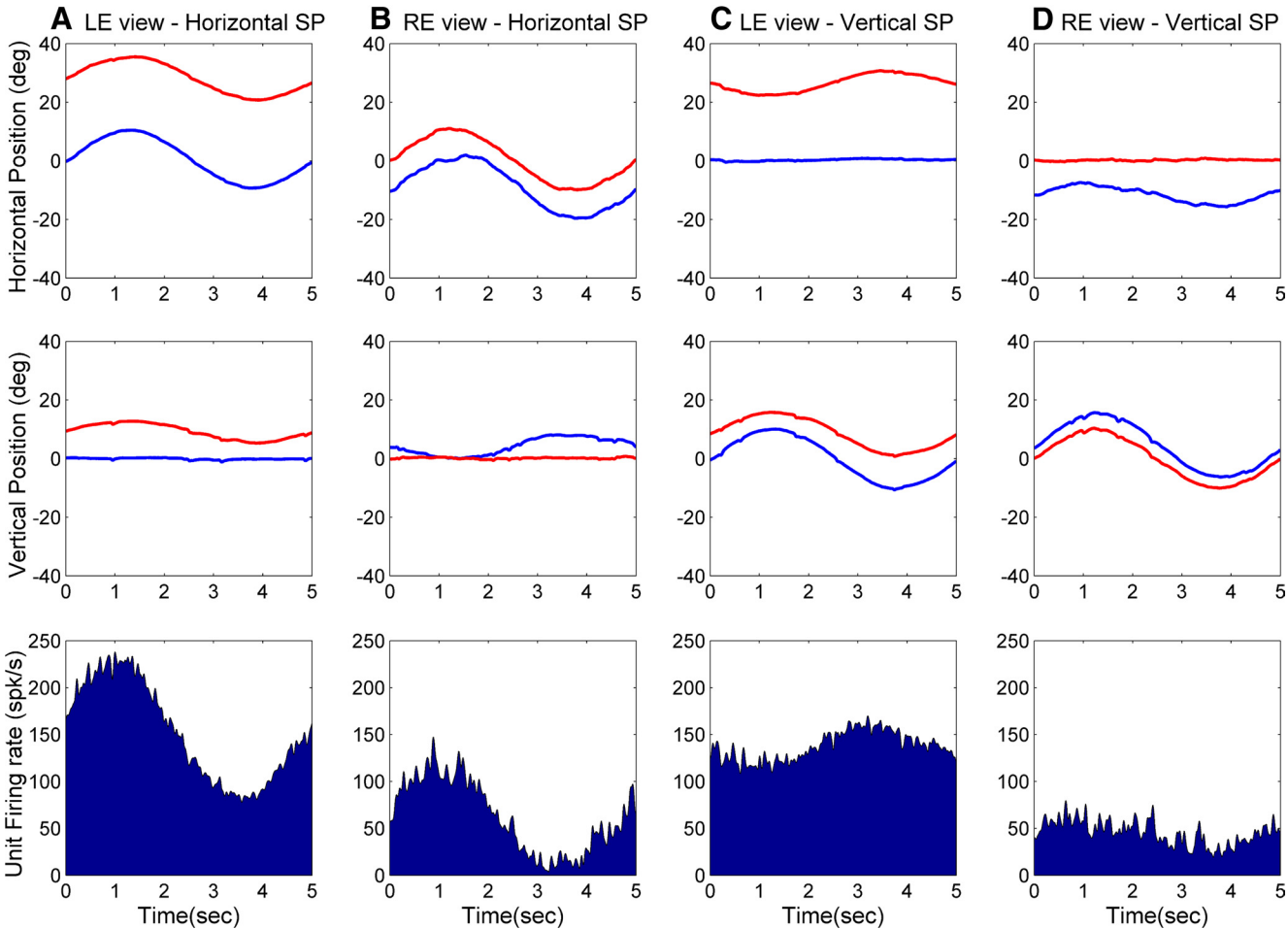
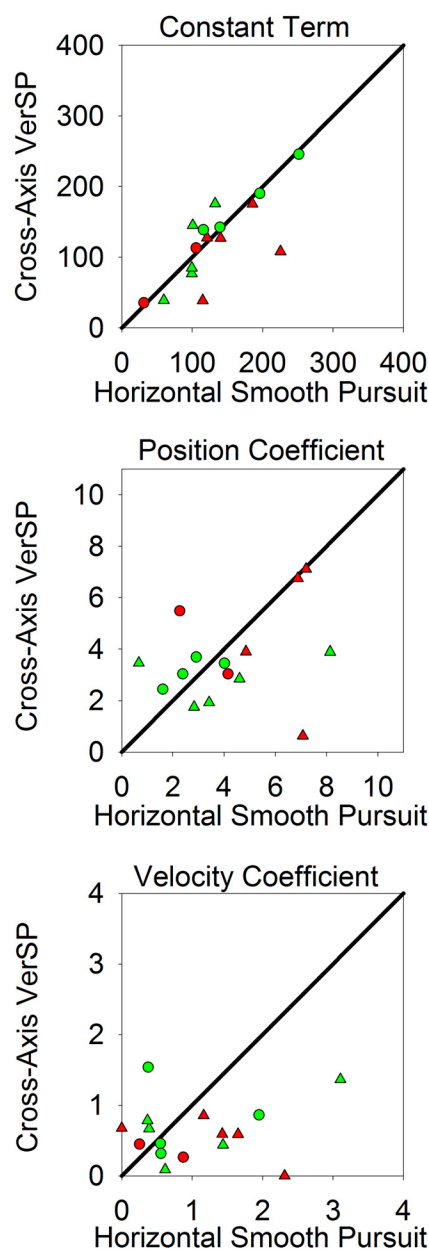


FIGURE 5. Single-unit activity in a sample binocular motoneuron that was sensitive to rightward eye movements (RTBT motoneuron recorded from left OMN). We observed significant modulation of activity during all four tracking conditions, including during vertical tracking with the left eye viewing (C), when only the right eye shows a horizontal cross-axis component. Binocular fit equations obtained for the horizontal and vertical tracking conditions with combined left eye and right eye viewing data are as follows. (A) and (B):  $FR(t) = 4.60E_H(t) + 0.39E_V(t) + 1.78E_C(t) + 1.98E_C(t) + 100$ ; CD = 0.98. (C) and (D):  $FR(t) = 2.85E_H(t) + 0.67E_V(t) + 2.31E_C(t) + 1.23E_C(t) + 77$ ; CD = 0.99.



**FIGURE 6.** Comparison of position ( $K_p$ ), velocity ( $R_p$ ), and constant ( $C$ ) coefficients during horizontal tracking versus cross-axis horizontal component during vertical tracking. On the x-axis are estimated parameter values obtained from the model fits for horizontal smooth tracking with left and right eye viewing data combined. On the y-axis are estimated parameter values obtained from the model fit for the horizontal component during vertical tracking with left and right eye viewing data combined. Color legends as in Figure 4.

new resting lengths conform to the postsurgical eye position. The implication of muscle length adaptation is that the unbalanced neural activity that initially drove the strabismus can return to a “normal” state once the muscles have altered their lengths. Similarly, Guyton and colleagues<sup>14,15,26</sup> suggested that changes in vergence tonus in strabismus drive muscle length adaptation, in turn decreasing the need for chronic changes in vergence tonus. In a Hering framework, vergence tonus can be interpreted as that part of motoneuron innervation of EOM that is due to inputs from premotor vergence-related areas such as the supraoculomotor area (SOA).<sup>27,28</sup> Therefore, when viewing a straight-ahead target (0°) at a fixed distance, a part of the firing rate of the MRMN

would be due to premotor vergence input. In a modeling sense, motoneuron responses are best fit with a binocular model (i.e., with both right and left eye terms in the model). Note that the binocular right eye/left eye model is mathematically equivalent to a conjugate/vergence model for motoneuron responses wherein the cells exhibit different sensitivities to conjugate and vergence positions.<sup>29–31</sup> Therefore, vergence tonus likely also constitutes a part of the position sensitivity of a motoneuron. King and Zhou<sup>32</sup> have also suggested that part of the position signal in the motoneurons arises from SOA input.

Potentially, muscle length adaptation driven by chronic changes in vergence tonus could also occur in the AMO exotropes. This might take the form of a permanent shortening of the lateral rectus and lengthening of the medial rectus of one or perhaps both eyes followed by the return of the brain (motoneurons) to “normal” states of innervation. Under these circumstances, if the animal is forced to fixate with the “adapted” eye, then the brain must supply increased innervation to the medial rectus muscle from MRMNs and decreased innervation to the lateral rectus muscle from the lateral rectus motoneurons (LRMNs) of that eye to compensate for the lengthened state of the medial rectus muscle and shortened state of the lateral rectus muscle. When applying the model fits to such a population of MRMN cells, the additional innervation should manifest as an increase in the constant term (“ $C$ ”) and as an increase in the position (“ $K$ ”) sensitivity of the population when compared with the MRMN population of a normal animal. We did not observe any such fundamental changes in motoneuron sensitivity. The average sensitivities of the horizontal motoneurons in our sample estimated during horizontal tracking are shown in Table 1. These parameter values generally agree with those identified in normal monkey studies of MRMN activity by other investigators, although not all these studies used the same experimental conditions as ours to estimate neuronal sensitivities. Thus, Gamlin and Mays<sup>29</sup> reported values of  $K_c$  (conjugate position sensitivity) =  $5.4 \pm 1.7$  spikes  $\cdot$  s<sup>-1</sup>  $\cdot$  deg<sup>-1</sup>;  $K_v$  (vergence position sensitivity) =  $6.1 \pm 5.1$  spikes  $\cdot$  s<sup>-1</sup>  $\cdot$  deg<sup>-1</sup>;  $R_v$  (vergence velocity sensitivity) =  $1.52 \pm 1.75$  spikes  $\cdot$  s<sup>-1</sup>  $\cdot$  deg<sup>-1</sup>  $\cdot$  s<sup>-1</sup>;  $C$  =  $79 \pm 41$ , Mays and Porter<sup>28</sup> reported values of  $K_c$  =  $4.6 \pm 1.3$  spikes  $\cdot$  s<sup>-1</sup>  $\cdot$  deg<sup>-1</sup>;  $K_v$  =  $2.6 \pm 2.6$  spikes  $\cdot$  s<sup>-1</sup>  $\cdot$  deg<sup>-1</sup>;  $R_c$  =  $0.96 \pm 0.03$  spikes  $\cdot$  s<sup>-1</sup>  $\cdot$  deg<sup>-1</sup>  $\cdot$  s<sup>-1</sup>;  $R_v$  =  $0.74 \pm 0.24$  spikes  $\cdot$  s<sup>-1</sup>  $\cdot$  deg<sup>-1</sup>  $\cdot$  s<sup>-1</sup>;  $C$  =  $100 \pm 40$  spikes/s. Van Horn and Cullen<sup>33</sup> reported sensitivity coefficients of  $K_c$  =  $6.2 \pm 2.67$  spikes  $\cdot$  s<sup>-1</sup>  $\cdot$  deg<sup>-1</sup>;  $R$  =  $0.53 \pm 0.32$  spikes  $\cdot$  s<sup>-1</sup>  $\cdot$  deg<sup>-1</sup>  $\cdot$  s<sup>-1</sup>;  $C$  =  $111 \pm 33$  spikes/s. Recently, Miller and colleagues<sup>34</sup> reported a mean  $K_c$  value of 4.34 spikes  $\cdot$  s<sup>-1</sup>  $\cdot$  deg<sup>-1</sup> and a  $K_v$  value of 5.68 spikes/s. In our study, the regression coefficients reported in Table 1 are a combination of the conjugate and vergence sensitivities of the motoneurons.

Therefore, our data do not appear to support the muscle length adaptation hypothesis. Rather the data suggest that the moment-by-moment determination of strabismus angle is primarily carried out by neural innervation. However, it should be noted that the relationship between motoneuron firing, muscle contraction and the torque produced at the tendon to generate a rotational eye movement is quite complex and not yet fully understood. One prominent finding, yet unresolved, is that both LRNM and MRMN responses differ when the eye attains a certain position in the orbit by a conjugate eye movement versus a vergence eye movement.<sup>29,34</sup> However, these observations of motoneuron sensitivity differences between vergence and conjugate eye movements are not accompanied by equivalent predictions of force changes in lateral and medial rectus muscles.<sup>34</sup> Additionally, the EOM has six different fiber types and it appears that the singly innervated fibers (SIFs) and the multiply innervated fibers (MIFs) might be differentially active during fast eye movements such as saccades and slow eye movements such as vergence. Further, SIFs and MIFs appear to be innervated by different motoneuron subgroups within the same motor nucleus,<sup>35</sup> although no data exist



TABLE 2. Population Characteristics of MRMNs during Cross-Axis Movements (mean  $\pm$  standard deviation)

Parameter	Horizontal Smooth Pursuit	Horizontal Component during Vertical Tracking
Ipsi position coefficient, $K_i$	$4.72 \pm 3.02$	$3.54 \pm 1.71$
Ipsi velocity coefficient, $R_i$	$1.07 \pm 0.86$	$0.62 \pm 0.41$
Contra position coefficient, $K_c$	$-0.44 \pm 3.13$	$0.45 \pm 2.14$
Contra velocity coefficient, $R_c$	$0.69 \pm 0.8$	$0.43 \pm 0.68$
Constant, $C$	$132.58 \pm 57.68$	$122.67 \pm 58.83$
Coefficient of Determination, CD	$0.87 \pm 0.19$	$0.83 \pm 0.13$

Subscripts: i, ipsilateral eye coefficient; c, contralateral eye coefficient.

of whether the response characteristics of neurons innervating SIFs is different from that of neurons that innervate MIFs. Given some of these complex and potentially confounding factors, it is impossible to completely exclude any secondary contribution from muscle length adaptation toward the maintenance of the strabismic state. Perhaps direct anatomic studies of EOM including detailed analysis of the different muscle fiber types would help to confirm or reject our conclusion that muscle length adaptation plays at most a minor role in setting the state of a sensory-induced strabismus. We also speculate that muscle length adaptation could play a more prominent role in types of strabismus wherein one of the eyes is also deeply amblyopic and therefore is always the nonfixating and deviated eye. This situation is possibly most similar to the preparation of Scott<sup>13</sup> in that a particular eye always assumes a deviated position. The AMO paradigm does not lead to particular eye preference and the monkeys freely alternate their eye of fixation during binocular viewing.<sup>6</sup>

### Relationship between MRMN Activity and Horizontal Cross-Axis Movements

Previously we showed that activity of vertical BT neurons in the OMN was driving the inappropriate vertical cross-axis movement observed during horizontal tracking.<sup>8</sup> This study complements the previous results and shows that, in AMO monkeys, MRMNs drive the horizontal cross-axis movements (that lead to "A" patterns) observed during a vertical tracking task. When comparing the model coefficients during the different tracking conditions (i.e., horizontal smooth pursuit versus horizontal component during vertical smooth pursuit [cross-axis tracking]), we found no statistical differences in position and velocity coefficients or the constant term (Fig. 6). However, we observed substantial scatter of the coefficient estimates in the comparison conditions. Although, it did not arise to statistical significance, the velocity coefficient comparison in Figure 6 suggests a skew toward the x-axis. Scatter of coefficient estimates was also observed in the analysis of horizontal misalignment shown in Figure 4. There are several possible sources for the scatter. It could indicate a missing term in the model equation that represents the mechanics of the eye plant in the orbit with contributions from the pulleys. Also, variables such as eye accommodation or position in the orbit were not controlled for and these might have contributed to the variability in coefficient estimates. King and Zhou<sup>32</sup> proposed a model in which different premotor areas (SOA and abducens internuclear neurons in particular) contribute differently toward the position and velocity components of MRMN responses during vergence and conjugate eye movements. It is possible that these premotor areas contribute differently in the tracking conditions tested in this study because of the varied eccentric locations of the eye when it is viewing or when covered. Such a framework could allow apparent changes in the velocity coefficient during the cross-axis condition but not the position coefficient, as was the tendency in the strabismic monkeys. A recent study has identified the presence of com-

partmental organization within horizontal recti along with independent innervation of these compartments.<sup>36</sup> It is possible that these compartments affect eye movements slightly differently when the eye to which the muscle projects is eccentric in the orbit, thereby affecting the coefficient estimates and contributing to the scatter. In any case, considering the population activity as a whole it appears that the primary determinant to the horizontal cross-axis movements is indeed neural in the AMO monkey.

Our data also argue against a role of static ocular torsion in producing A/V patterns in these AMO animals.<sup>15</sup> Thus Guyton and Weingarten<sup>10</sup> proposed that a static torsion of the non-viewing eye could result in a change in the pulling direction of the rectus muscles. Under this hypothesis, contraction of vertical rectus muscles results in an inappropriate horizontal eye movement and contraction of horizontal rectus muscles results in an inappropriate vertical eye movement. Therefore, we would expect activity in vertical motoneurons to correlate with the horizontal component of cross-axis movements ("A" patterns) and activity in horizontal motoneurons to correlate with the vertical component of cross-axis movements (DVD). In fact, we observed just the reverse in that horizontal motoneurons appear to drive horizontal component of cross-axis movements (this study) and vertical motoneurons appear to drive vertical component of cross-axis movements.<sup>8</sup>

### Possible Sources for Neural Drive for Misalignment and Cross-Axis Movements

The correlation between the horizontal motoneuron activity and state of horizontal misalignment and also the inappropriate horizontal cross-axis component does not imply that these strabismus properties are generated at the level of the motoneurons. It is likely that premotor areas are the source of the signals that set the state of strabismus. Perhaps the SOA plays a role in maintaining the state of horizontal misalignment. The SOA cells monosynaptically project to the MRMNs and respond to a change in eye vergence.<sup>27</sup> and some are shown to carry strabismic angle information (Das VE. *IOVS* 2010;51:ARVO E-Abstract 2997). Recent anatomic studies have shown that MRMNs receive projections from premotor structures associated with vertical and torsional eye movement structures and these could be the source for cross-axis function.<sup>37</sup>

### Binocular Encoding in Medial Rectus Motoneurons

In our sample, we found that 57% of motoneurons showed binocular encoding. This finding is consistent with previously reported data on binocular motoneurons in the OMN and abducens nucleus.<sup>21,22,31,33</sup> It is not clear how or why such binocular encoding is observed, although it may simply reflect the varied monocular and binocular inputs to the motoneurons.<sup>22,23,31,38</sup> Some have suggested that the contralateral component is eliminated when considering population character-



istics of motoneurons or that perhaps there is some selective synaptic weighting that minimizes contribution of binocular cells toward generation of an eye movement.<sup>21</sup> Examination of the contralateral eye coefficients in our study shows that the mean values are close to zero, suggesting that the population effect of contralateral eye encoding is indeed rather weak. Given the uncertainty in the significance of contralateral eye encoding, we mainly compared the ipsilateral coefficients obtained from the model fit for the second part of the analysis focused on cross-axis function. However, statistical testing indicated that the contralateral eye component also did not show significant differences between horizontal pursuit and cross-axis function.

### Acknowledgments

The authors thank Michael Mustari for help with surgical implantation and Michelle Swann for technical assistance.

### References

- Boothe RG, Dobson V, Teller DY. Postnatal development of vision in human and nonhuman primates. *Annu Rev Neurosci.* 1985;8:495–545.
- Das VE, Fu LN, Mustari MJ, Tusa RJ. Incomitance in monkeys with strabismus. *Strabismus.* 2005;13:33–41.
- Crawford ML, von Noorden GK. Optically induced concomitant strabismus in monkeys. *Invest Ophthalmol Vis Sci.* 1980;19:1105–1109.
- Economides JR, Adams DL, Jocson CM, Horton JC. Ocular motor behavior in macaques with surgical exotropia. *J Neurophysiol.* 2007;98:3411–3422.
- Tusa RJ, Mustari MJ, Das VE, Boothe RG. Animal models for visual deprivation-induced strabismus and nystagmus. *Ann NY Acad Sci.* 2002;956:346–360.
- Das VE. Alternating fixation and saccade behavior in nonhuman primates with alternating occlusion-induced exotropia. *Invest Ophthalmol Vis Sci.* 2009;50:3703–3710.
- Fu L, Tusa RJ, Mustari MJ, Das VE. Horizontal saccade disconjugacy in strabismic monkeys. *Invest Ophthalmol Vis Sci.* 2007;48:3107–3114.
- Das VE, Mustari MJ. Correlation of cross-axis eye movements and motoneuron activity in non-human primates with “A” pattern strabismus. *Invest Ophthalmol Vis Sci.* 2007;48:665–674.
- Guyton DL. Dissociated vertical deviation: etiology, mechanism, and associated phenomena. Costenbader Lecture. *J Am Assoc Pediatr Ophthalmol Strabismus.* 2000;4:131–144.
- Guyton DL, Weingarten PE. Sensory torsion as the cause of primary oblique muscle overaction/underaction and A- and V-pattern strabismus. *Binocul Vis Strabismus Q.* 1994;9:209–236.
- Oh SY, Clark RA, Velez F, Rosenbaum AL, Demer JL. Incomitant strabismus associated with instability of rectus pulleys. *Invest Ophthalmol Vis Sci.* 2002;43:2169–2178.
- Das VE. Investigating mechanisms of strabismus in nonhuman primates. *J Am Assoc Pediatr Ophthalmol Strabismus.* 2008;12:324–325.
- Scott AB. Change of eye muscle sarcomeres according to eye position. *J Pediatr Ophthalmol Strabismus.* 1994;31:85–88.
- Guyton DL. The 10th Bielschowsky Lecture. Changes in strabismus over time: the roles of vergence tonus and muscle length adaptation. *Binocul Vis Strabismus Q.* 2006;21:81–92.
- Guyton DL. Ocular torsion reveals the mechanisms of cyclovertical strabismus: the Weisenfeld lecture. *Invest Ophthalmol Vis Sci.* 2008;49:846–857.
- Das VE, Ono S, Tusa RJ, Mustari MJ. Conjugate adaptation of saccadic gain in non-human primates with strabismus. *J Neurophysiol.* 2004;91:1078–1084.
- Judge SJ, Richmond BJ, Chu FC. Implantation of magnetic search coils for measurement of eye position: an improved method. *Vision Res.* 1980;20:535–538.
- Richmond BJ, Optican LM, Podell M, Spitzer H. Temporal encoding of two-dimensional patterns by single units in primate inferior temporal cortex. I. Response characteristics. *J Neurophysiol.* 1987;57:132–146.
- Sylvestre PA, Cullen KE. Quantitative analysis of abducens neuron discharge dynamics during saccadic and slow eye movements. *J Neurophysiol.* 1999;82:2612–2632.
- Clandiel RA, Mays LE. Characteristics of antidromically identified oculomotor internuclear neurons during vergence and versional eye movements. *J Neurophysiol.* 1994;71:1111–1127.
- Sylvestre PA, Cullen KE. Dynamics of abducens nucleus neuron discharges during disjunctive saccades. *J Neurophysiol.* 2002;88:3452–3468.
- Zhou W, King WM. Premotor commands encode monocular eye movements. *Nature.* 1998;393:692–695.
- Sylvestre PA, Choi JT, Cullen KE. Discharge dynamics of oculomotor neural integrator neurons during conjugate and disjunctive saccades and fixation. *J Neurophysiol.* 2003;90:739–754.
- Christiansen S, Madhat M, Baker L, Baker R. Fiber hypertrophy in rat extraocular muscle following lateral rectus resection. *J Pediatr Ophthalmol Strabismus.* 1988;25:167–171.
- Christiansen SP, McLoon LK. The effect of resection on satellite cell activity in rabbit extraocular muscle. *Invest Ophthalmol Vis Sci.* 2006;47:605–613.
- Wright WW, Gotzler KC, Guyton DL. Esotropia associated with early presbyopia caused by inappropriate muscle length adaptation. *J Am Assoc Pediatr Ophthalmol Strabismus.* 2005;9:563–566.
- Mays LE. Neural control of vergence eye movements: convergence and divergence neurons in midbrain. *J Neurophysiol.* 1984;51:1091–1108.
- Mays LE, Porter JD. Neural control of vergence eye movements: activity of abducens and oculomotor neurons. *J Neurophysiol.* 1984;52:743–761.
- Gamlin PD, Mays LE. Dynamic properties of medial rectus motoneurons during vergence eye movements. *J Neurophysiol.* 1992;67:64–74.
- King WM, Zhou W. Neural basis of disjunctive eye movements. *Ann NY Acad Sci.* 2002;956:273–283.
- King WM, Zhou W, Tomlinson RD, et al. Eye position signals in the abducens and oculomotor nuclei of monkeys during ocular convergence. *J Vestibul Res.* 1994;4:401–408.
- King WM, Zhou W. New ideas about binocular coordination of eye movements: is there a chameleon in the primate family tree? *Anat Rec.* 2000;261:153–161.
- Van Horn MR, Cullen KE. Dynamic characterization of agonist and antagonist oculomotoneurons during conjugate and disjunctive eye movements. *J Neurophysiol.* 2009;102:28–40.
- Miller JM, Davison RC, Gamlin PD. Motor nucleus activity fails to predict extraocular muscle forces in ocular convergence. *J Neurophysiol.* 2011;105:2863–2873.
- Buttner U, Buttner-Ennever JA. Present concepts of oculomotor organization. *Prog Brain Res.* 2006;151:1–42.
- da Silva Costa RM, Kung J, Poukens V, Yoo L, Tychsen L, Demer JL. Intramuscular innervation of primate extraocular muscles: unique compartmentalization in horizontal recti. *Invest Ophthalmol Vis Sci.* 2011;52:2830–2836.
- Ugolini G, Klam F, Doldan Dans M, et al. Horizontal eye movement networks in primates as revealed by retrograde transneuronal transfer of rabies virus: differences in monosynaptic input to “slow” and “fast” abducens motoneurons. *J Comp Neurol.* 2006;498:762–785.
- Waitzman DM, Van Horn MR, Cullen KE. Neuronal evidence for individual eye control in the primate cMRF. *Prog Brain Res.* 2008;171:143–150.